SIN-CHN
SCIENTIFIC PRESS PTE.LTD.

Molecular & Cellular Biomechanics 2025, 22(3), 886.
https://doi.org/10.62617/mcb886

Article

Research on prediction and estimation of operational states of power electronic equipment in bioreactor fields based on discrete Kalman filter algorithm and biomolecular markers

Junjie Liu[1,2,*], Pingping Zhang[1,2]

[1] School of Hebi Institute of Engineering and Technology, Henan Polytechnic University, Hebi 458000, China
[2] Department of Preparation Division, Henan Institute of Information Technology, Hebi 458000, China
*** Corresponding author:** Junjie Liu, liujunjieemail@163.com

CITATION

Liu J, Zhang P. Research on prediction and estimation of operational states of power electronic equipment in bioreactor fields based on discrete Kalman filter algorithm and biomolecular markers. Molecular & Cellular Biomechanics. 2025; 22(3): 886. https://doi.org/10.62617/mcb886

ARTICLE INFO

Received: 21 November 2024
Accepted: 13 January 2025
Available online: 24 February 2025

Abstract: The prediction and evaluation of the states of electronic and electrical equipment hold significant research value across various fields. Kalman filter algorithm is used to identify, predict and estimate the parameters of some electronic components in the electronic equipment are tested. Rate the common failure level, adjust the appropriate Kalman filter algorithm, to ensure that the electronic equipment is always in the best operation state, and can avoid the damage of power engineering equipment. Biological thermal response significantly impacts the thermal management of electronic devices. By simulating the thermal conductivity of biological tissues, the heat dissipation design is optimized to ensure device temperature remains below the thermal damage threshold. The expression of Heat Shock Proteins (HSP) and cell viability serve as biomarkers to evaluate the thermal effects of devices on biological tissues, enhancing safety and reliability. This paper discusses the necessity of prediction and estimation of power devices, and then combines the actual scientific research, mainly for the temperature of semiconductor power devices and the DC (Direct Current) voltage of the main circuit of the inverter, from the mathematical model, the realization of state prediction algorithm and thermal effects of devices on biological tissues. This study effectively avoids damage and failures caused by high temperatures, addresses the challenge of output voltage accuracy in complex environments, and offers new insights into equipment states estimation from a biomechanical perspective, thereby enhancing safety and reliability.

Keywords: the Kalman filtering algorithm; power electronic equipment; forecast and estimation; Heat Shock Protein (HSP); biological tissue thermal conductivity; biomechanics; biomolecular

1. Introduction

1.1. Background of power electronic equipment

The operation reliability of electronic equipment is not only in the national defense security, aviation company and other high-tech equipment industry, but also in the commercial and home products industry has become the focus of attention. Especially so far, with the volume and quality of power engineering electronic equipment more and more light and effective, the specific content of standard storage is constantly improving, the level of intelligence is becoming more and more fierce, the reliability of electronic equipment at work also follows the development trend [1].

During the Second World War, Germany wanted to achieve the development strategy of airstrikes against London with missiles, but most of the missiles were abnormal on the launch tower due to common faults caused by electronic equipment,

and some missiles burst into the sea before reaching London. Similarly, more than half of the high-definition aerial radio stations sent to HTC (High Technology Center) were damaged during transportation and storage, causing serious damage. But, according to U.S. Special Forces reports, the surviving electronics are only half the normal ones working efficiently. During this time, more than 2000 aircraft were lost due to the reliability of the equipment, more than double the number of normal unfortunate victims. A large amount of budget, human and network resources are invested into reliability experiments. With the use of electronic equipment in military forces, electronic communication equipment, road traffic safety equipment, diagnosis and treatment scientific research equipment, power and electrical equipment and space science become more complex, and destroyed, the rate of equipment is increased, and the reliability of new products of electronic equipment will be higher and higher [2]. As shown in **Figure 1**.

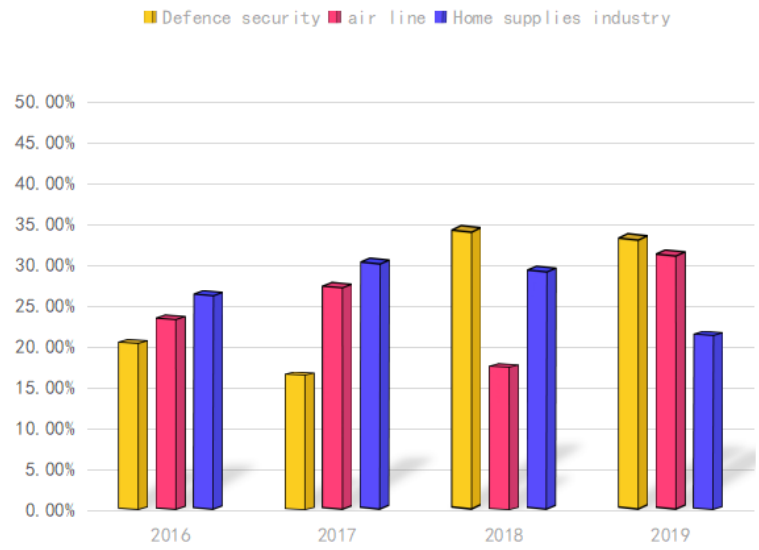

Figure 1. Error rate of power electronic equipment in various fields.

1.1.1. The importance of the reliability of power electronic equipment

The loss caused by the mechanical failure is very great. A U.S. space satellite was destroyed after some electronic failure, causing $2.2 million in damage. In 1971, three Soviet cosmonauts were killed in a damaged spacecraft. The U.S. military uses a computer to monitor military training. Because of the common computer failure, the order of the soldiers has changed, leading to the confusion. Because the computer failed during take-off, American troops fired cruise missiles from his plane, leading to a major plane crash. Three common rocket failures in 1979 caused more than $100 million in damage to the U.S. space department. A leak at the Three Mile Island nuclear power plant in the United States caused the failure of the refrigeration compressor valve, causing an international crisis. In conclusion, many similar cases are proposed to determine the safety measures of electronic equipment [3].

The rapid development of electrical equipment continues. From the first generation of electrical equipment to the second generation of electrical equipment, and today from this small scale of electrical equipment to specifications, combined together. With the rapid development of electronic equipment miniaturization, the rate

of machinery and equipment, the temperature of the internal structure increase, and the thermal conductivity decrease. The reliability of the electrical equipment decreases with the rise in temperature. Therefore, the reliability of electronic products has attracted much attention. As shown in **Table 1**.

Table 1. More and more attention is being paid to the reliability of electronic equipment.

The loss of poor reliability is very serious.	**A $2 component disabled the entire satellite, with a loss of $2.2 million.**
In 1963, American aviation aircraft had 1.46 accidents for every 10,000 h flown.	Electronic products are developing towards miniaturization and miniaturization direction.
The result is an increasing device density.	Therefore, the reliability of electronic components has been paid great attention to by people.

1.1.2. The importance of reliability protection of power electronic equipment

For ordinary equipment, when there is a problem, maintenance can be selected, and the time is not as emergency as military electronic device equipment, but for military goods, it has long been impossible to shut down in public for maintenance, especially in emergency operations. Perhaps it is the high error rate that makes many soldiers more and more excessively passive [4]. The rapid development of modern war gives a higher demand for military electrical and electronic equipment.

All this shows that it is important to maintain the stability of electronics. Since the 1990s, we can see that the more reliable equipment can withstand the harsh discipline in the war and the environment, and the idea of treating the equipment is also subtly changing and becoming more and more critical. From the original after the inspection, strengthen testing, into a new starting point in the bud. From the perspective of scientific and practical thinking, the solutions described in the paper should adopt a new thinking mode to meet the requirements of reform, development and market competition. As shown in **Figure 2**.

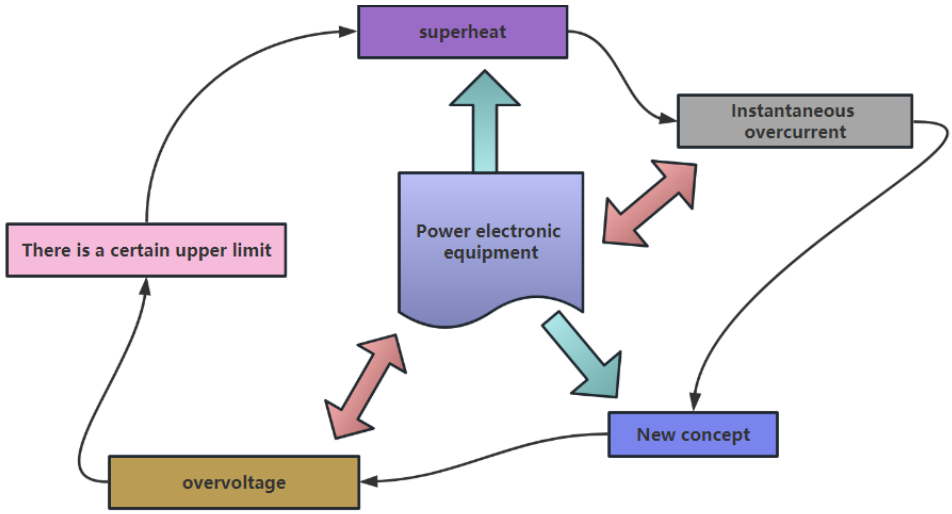

Figure 2. Development history of electronic equipment.

1.2. Background of Kalman filtering

The Kalman filter mode has the characteristics of data information estimation and non-improvement estimation, and this advantage plays a decisive role in the

application of electronic and electrical equipment. It can collect sensor data and information to solve electronic devices, and get the most accurate and more reliable information than a single sensor. Power electronics is studied in the discrete system, and the Kalman filter algorithm combined with the power device are presented. Depending to the composition of these two elements improves the performance of electronic devices.

1.2.1. Application and development of discrete Kalman filtering

In communication, radar detection, automation technology and other industries, the Kalman filter can be used to calibrate the wave type of the signal, and the state can also be inferred according to the signal polluted by noise. For example, this prediction has some problems such as aircraft range prediction, radar detection and tracking prediction, automation technology, and weather forecast, and can be solved by using the basic theory of Kalman filter [5].

The Kalman filter optimization algorithm is derived from publicly published research papers. Kalman solved the filtering problem of discrete system technically with iterative update in the 20th world and 60th period [6]. This exploration and discovery are today called the Kalman filter method. Kalman filtering is very powerful and versatile. Kalman filtering can predict not only the present and former state of the signal, but also the future state. As shown in **Figure 3**.

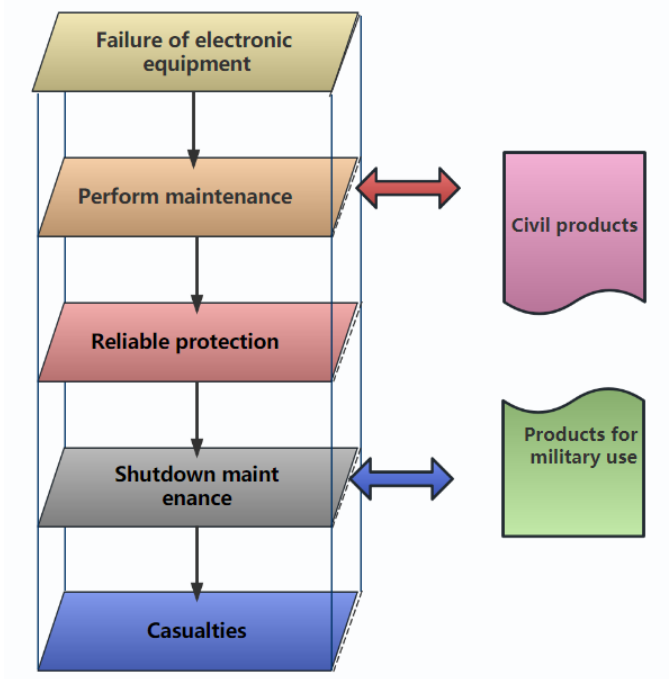

Figure 3. Application prospect of the Kalman filter.

The minimum RMSE (Root Mean Square Error) was used as a parameter assessed by the Kalman filter. State space represents the signal intensity ratio model for the initial sample, current value and observations used by the Kalman filter algorithm in measuring different signal states.

The Kalman filter algorithms have been used in many industries for several decades. Experience has proved that the Kalman filter is the best solution, and sometimes even the best and most effective solution, when solving the problem of

power electronic equipment [7]. The Kalman filter algorithm is applied in the fields of electronics, control, navigation, wireless sensor network and other fields. It is widely used in many fields. In many military applications, such as radar tracking, passive position tracking, and missile tracking, the Kalman filter algorithm has achieved good results and improved very well. As shown in **Table 2**.

Table 2. The Kalman filter is widely used.

In communication, radar, automatic control and other wave control, the waveform can be used to restore or estimate the state of the signal from the signal polluted by noise.	The Kalman filter algorithm first follows the academic paper published by Mr. Kalman to solve the problem of discrete linear filter in 1960.	Using the Kalman filter method, we can not only predict the current and past states of the signal.
The Kalman filter algorithm has been used in various industries for more than 30 years.	The Kalman filter algorithm is now widely used, including in electronics, control, navigation, wireless sensor network and other fields.	Such prediction and estimation can be done without knowing the exact model of the system.

1.2.2. Characteristics of the discrete Kalman filtering

The structure of the Kalman filter depends on the state expression and observed expression using different matrices. With the change of sound decibel and analysis noise matrix, the state transfer and analysis matrix are able to change over time [8]. Therefore, the Kalman filter is suitable not only for estimating different states of stable and random event processes, but also to predicting different states of unrandom events processes in the analysis space vector. This gives it a wide range of applications.

Because Kalman filter is a recursive algorithm prediction, the data information storage cost is small and the accounting cost is small, which prevents the advanced matrix inverse problem. The filtered gain value matrix and analysis are irrelevant, which can realize offline calculation, reduce the cost of online real-time online analysis, and enhance the waiting time [9]. The discrete variable Kalman filter can not only obtain the state filter value and state estimation at the same time, but also obtain the mean square error matrix and state estimation of the filtered state at the same time, that is, retrieval, filtering and accurate evaluation. As shown in **Figure 4**.

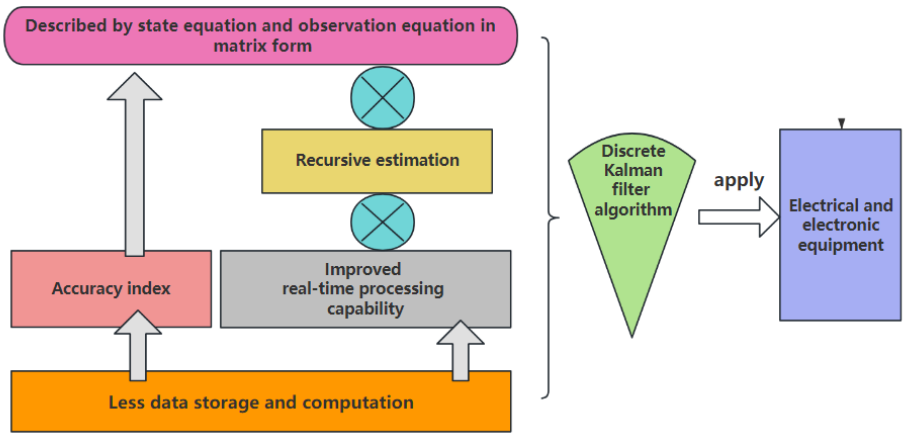

Figure 4. Advantages of the Kalman filtering.

1.2.3. Properties of the discrete Kalman filtering

The case filter value is the linear natural number of the RMSE error. Because this is an unbiased estimator, the filtered RMS error matrix is the smallest variance of all linear estimators. Filter gain matrix of hazard first two RMSE error matrix, noise variance matrix, and visual effect noise variance matrix.

With the increase of the cognitive noise variance matrix, the filter gain matrix instead decreases. Because the deviation of the new data varies with the improvement of audio analysis, the filter gain matrix must reduce the impact of audio analysis [10]. As the original rms error matrix shrinks, the filter gain matrix also shrinks. This means that the base estimate is good, the scale value is small, and the prediction value change is small. The square noise matrix has a small variance, which means that the data signal noise is relatively small and the filter gain matrix is relatively small, which benefits to the accurate prediction analysis. As shown in **Figure 5**.

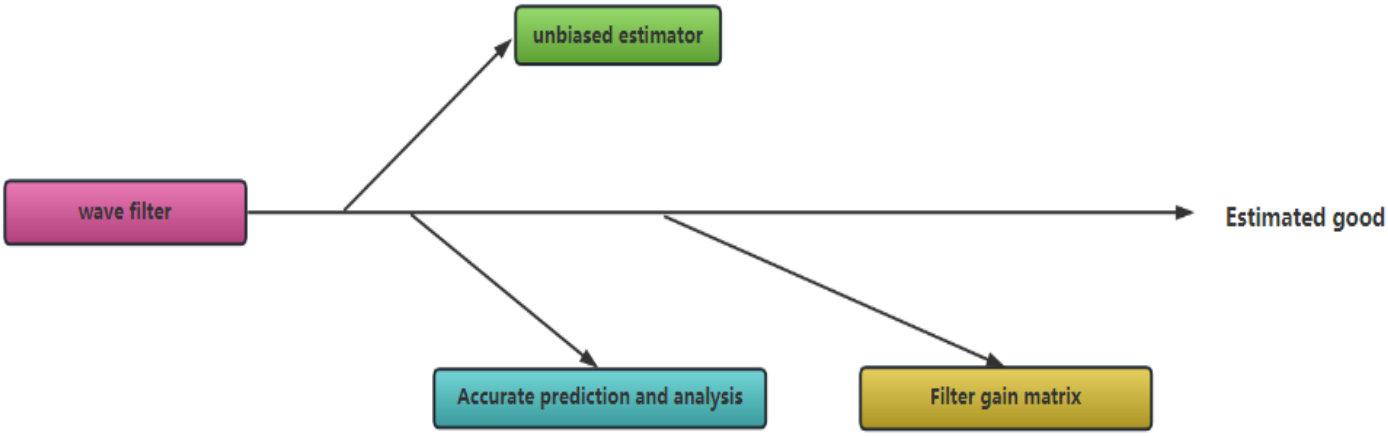

Figure 5. Observations.

1.3. Research background on the integration of biomechanics with the field of electrical and electronic devices

Research at the intersection of biomechanics and the field of electronic and electrical equipment is emerging as a multidisciplinary focal area. This integrative approach combines mechanical principles from biology with performance optimization of electronic devices, aiming to enhance functionality, reliability, and efficiency through biomimicry, intelligent monitoring, and adaptive technologies.

Biomechanics provides significant inspiration for the development of high-performance materials and devices. For example, conductive hydrogels, characterized by their high water content, modulus similar to biological tissues, and excellent ionic conductivity, have become crucial components in soft bioelectronics. By incorporating fillers such as carbon nanomaterials, conductive polymers, and metal-based nanomaterials into conductive hydrogels, their electrical performance can be enhanced while retaining their flexibility. This makes them suitable for applications in wearable sensors, neural interfaces, and other advanced technologies [11,12].

The integration of biomechanics and electronic devices has achieved remarkable progress in the domain of wearable electronics. For instance, devices like

smartwatches and fitness bands can monitor physiological parameters such as heart rate and blood pressure. Additionally, they utilize built-in sensors, such as accelerometers and gyroscopes, to analyze human movement and mechanical data, providing users with exercise guidance and health insights [13,14]. Furthermore, wearable electronic devices can harvest and convert biomechanical energy, paving the way for energy-efficient innovations [15,16].

2. Method

2.1. Power electronics forecast

2.1.1. Prediction of the electronic devices using Kalman filter

In a variety of applications, we often encounter electrical and electronic equipment due to the interference of various factors and no way to continuous and stable operation of serious time will appear shutdown. The failure of the power supply is usually caused by the irregular power supply, such as the sudden overcurrent, overvoltage, overheating and other reasons that lead to the inability to work normally. Whether for military or civilian equipment, the solution is always done by adding overheating, overvoltage, overcurrent and other protection. Clearly, this protection has some limitations. At that time, due to the limitations of the scientific environment, it was impossible to develop an intelligent way to ensure a sustainable, stable and reliable power supply of power equipment [17].

We know that most violations have a developmental process, such as residual heat, which must be maintained for some time to reach criticality. On the other hand, there are some intrinsic connections between the different forms. It is therefore proposed to use Kalman filters in today's measurement systems to measure and predict some important states of electrical equipment, and to predict the final state of these parameters after a period of time. And judge the degree of the operating system into the fault, and then identify the impact on protection and prevention in advance, to avoid failure and power failure, so that not only can ensure the safety and reliability of the equipment, but also to ensure the normal operation of electrical and electronic equipment. Always keep running in the best state, which can greatly improve the continuous development of the control program optimization. At the same time, the state prediction technology in the traditional overvoltage, overcurrent, short circuit, overheating and other protection measures on the basis of the reliability of electrical power equipment operation to an unprecedented new height. As shown in **Figure 6**.

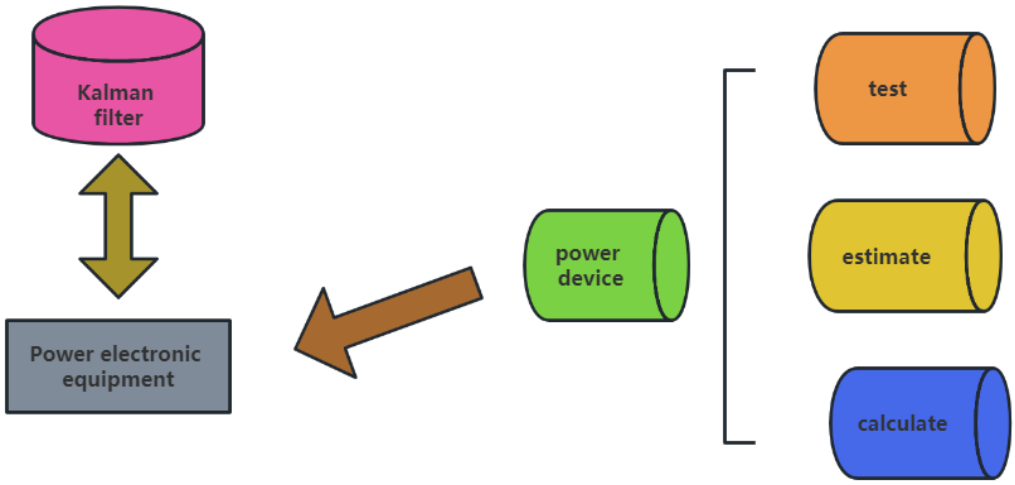

Figure 6. The prediction of the electronic device parameters.

2.1.2. Power consumption and heat dissipation of power and electronic equipment

When the ambient temperature of the electronic product continues to rise, the various functions of the heat dissipation device will be affected to varying degrees, and the temperature of the module will continue to rise at this time. Because of the characteristics of semiconductor components, with the increase of junction temperature, the self-destruction of semiconductor components will also increase. With the increase of temperature, a closed system space is formed. At the same time, increasing the coupling temperature limits the module operation by lowering the resistor. The state estimation method is based on the previous condition of many quantities and the value of the system state, and then according to the mutual relationship object structure, calculate the situation after the end of the operation. That is, the first evaluation, is to assess whether the actual operation is in the common fault area application and maintenance. This not only ensures the safety of the machine, but also allows the machine and equipment to play in its best condition [18]. These technologies, through current, short circuit faults and high-temperature protection, can improve power stability to a new level.

Changing the temperature of electrical equipment is the starting point of design and the two key factors to determine the safe operation of machinery and equipment. In repetitive work, the thyristor switches from off to off, then from on to on, and then closes again. According to the difference between the current and the voltage in the work, a certain amount of loss of kinetic energy will be generated. This includes through-state power consumption, reverse direction power consumption, through-state power consumption, broken state power consumption and positive middle power consumption.

Through the above, it is not difficult to find that the thyristor needs to cause great energy loss in the process of operation. This loss of energy will continuously convert into more heat, which will fall into an endless cycle and cause the temperature of the crystal triode to rise. When the temperature is too high. It makes the thyristor work difficult; it damages the temperature beyond the temperature. Therefore, moderate

temperature manipulation must be used for rapid and efficient digestion and absorption of heat, so that the junction temperature of the thyristor can be maintained in the category of normal operation [19].

The normal cooling mode is started by cooling: this kind of heat dissipation is achieved only by the material exchange between the radiator and the surrounding environment. It is all determined by the characteristics and temperature of the electric heater. Human factor cooling heat dissipation: can use the external various standards immediately absorb heat, to achieve the effect of heat dissipation. This condition can use some flow of wind or some cold water, or other substances, such as freon, for a little better effect. As shown in **Figure 7**.

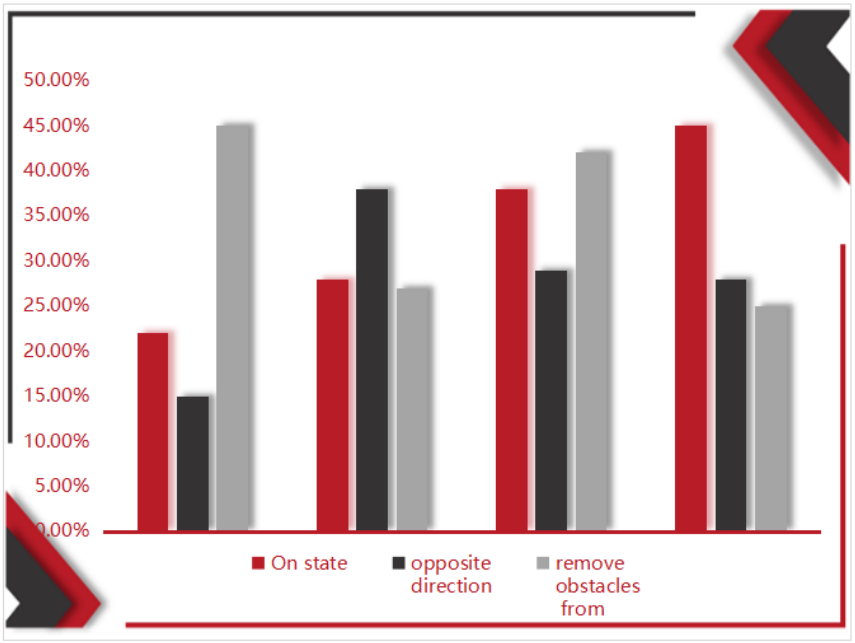

Figure 7. Dissipative power.

2.1.3. Equivalent thermal loop

The heat source is the thyristor matrix, because the dissipation power generated by the use will be gradually converted into energy to heat it up, which will greatly increase the temperature of the matrix. Heat will be transferred from all directions to the radiator, where the heat is distributed to the environment or dissipated through various media. Therefore, the heat transfer process includes various heat dissipation processes. A "thermal resistance" is usually used to indicate the transfer of this heat. Thermal resistance is the reciprocal of the thermal conductivity. For thermal resistance in semiconductor elements we can use *R*, the unit of thermal resistance is ℃/W [20]. Thermal resistance covers a wide range of almost all factors affecting the thermal conductivity, such as the thermal conductivity of materials and the environmental state of various components. The main way of heat dissipation design of electrical and electronic equipment is to design different heat dissipation mode and appropriate heat resistance radiator according to the different power input of the components, so that the temperature of the device chip is lower than the maximum rated junction temperature.

(1) Formula for calculating total thermal resistance:

$$R_{\text{total}} = \frac{T_j - T_a}{P} \tag{1}$$

where:

R_{total} is the total thermal resistance.

T_j is the junction temperature of the device chip.

T_a is the ambient temperature.

P is the input power.

(2) Thermal resistance decomposition formula:

$$R_{\text{total}} = R_{\text{substrate to case}} + R_{\text{case to heatsink}} + R_{\text{heatsink to ambient}} \tag{2}$$

where:

$R_{\text{substrate to case}}$ is the thermal resistance from the substrate to the case.

$R_{\text{case to heatsink}}$ is the contact thermal resistance from the case to the heatsink.

$R_{\text{heatsink to ambient}}$ is the thermal resistance from the heatsink to the ambient environment.

(3) Thermal resistance formula from shell to environment:

$$R_{\text{total}} = R_{\text{case to ambient}} + \frac{R_{\text{case to heatsink}} \times R_{\text{heatsink to ambient}}}{R_{\text{case to heatsink}} + R_{\text{heatsink to ambient}}} \tag{3}$$

where:

$R_{\text{case to ambient}}$ is the thermal resistance from the case directly to the ambient environment.

In practice, the total thermal resistance is usually divided into several different parts. The first part is the thermal resistance of the joint shell from the substrate to the shield layer, the second part is the contact thermal resistance from the shield layer to the radiator, and the third part is the so-called radiator from the radiator to the radiator environment. However, when considering the direct heat transfer from the shell to the environment, the total heat resistance has a more complex expression.

$$R_{ja} = R_{jc} + \frac{R_{ca}(R_{cs} + R_{sa})}{R_{ca} + R_{cs} + R_{sa}} \tag{4}$$

where R_{ja} for the total heat resistance, R_{jc} for a shell thermal resistance, R_{cs} for the contact thermal resistance, R_{sa} for the radiator thermal resistance [21].

As shown in **Table 3**.

Table 3. The basic data sheet.

Character	Parameter	Short-cut Process	Unit
T	Protect the temperature	100	℃
R_{cs}	Module to radiator heat resistance	0.5	℃/W
R_{sa}	Radiator to air heat resistance	1.0	℃/W
$T_{j\max}$	maximum temperature	60	℃

It can be seen that the smaller the thermal resistance, the lower the junction temperature rise, the better the heat dissipation effect. Similar to ohm's law in the DC

circuit, the temperature corresponds to the potential, dissipation power and current, and thermal resistance and resistance, respectively. Similar to the DC circuit.

2.1.4. Heat dissipation process

Due to the repeated action of the thyristor, the heat exchange is required each time. If the rectangular current pulse passes through the thyristor, the resulting dissipation power also has the shape of a rectangular pulse. The junction temperature change of the dissipative power supply is analyzed as follows. When the thyristor is fully engaged, the cathode will conduct electricity each time it is opened, and all the core heat will dissipate. The heat dissipation capacity of the thyristor is called the heat dissipation constant, and the heat dissipation constant is equal to the reciprocal of the thermal resistance. The junction temperature of the thyristor at a certain point is called the junction temperature.

Now consider the temporal variation of thermal energy changes. During this period, the heat energy generated by the substrate is dissipated by the heat sink. When the temperature of the mold increases, the heat capacity and the required heat energy are given by the following formula:

$$P_d \,\mathrm{d}t = K\Delta T_{jat} \,\mathrm{d}t + C_T \,\mathrm{d}\left(\Delta T_{jat}\right) \tag{5}$$

($P_d \,\mathrm{d}t$ for the heat energy generated by the pipe core, $K\Delta T_{jat} \,\mathrm{d}t$ for the heat energy dissipated by the radiator, $C_T \,\mathrm{d}\left(\Delta T_{jat}\right)$ for the heat energy needed).

The thyristor junction temperature increases exponentially with time. When the thyristor stops working and does not absorb the energy, the energy stored in the thyristor itself is released in the same variation pattern. If the power pulse appears in the background of zero power consumption, it is the ambient temperature; if the power pulse occurs in the background of constant power consumption of the device itself, it should be noted that the junction temperature is constant under constant power consumption. If several rectangular current pulses flow through the thyristor, the resulting dissipation power is also in the form of a continuous rectangular pulse **错误！未找到引用源。**. Of course, the greater the thermal inertia of the thermal system, the greater the thermal time constant, and the shorter the continuous duty cycle of the pulse, which can be considered as a pulse. As shown in **Table 4**.

Table 4. Heat dissipation properties of the thyristor.

When the thyristor work is repeated, a heat exchange is conducted for each opening and shutdown.	The heat energy generated by the pipe core during the period is dissipated by the radiator.	The junction temperature rise of the thyristor increases according to the exponential rule of time.
The energy accumulated in the thyristor itself will be released in the same changing pattern.	If multiple square wave current pulses flow in the thyristor, the dissipated power generated is also in the form of a continuous square wave pulse.	At some point, the junction temperature of the gate tube is called the transient junction temperature.

In the high-frequency pulse, the continuous pulse that is not enough to restore the joint temperature to the normal original temperature interval is caused. In the first several pulse cycles, because the starting point of the joint temperature rise caused by the subsequent increase of the pulse rises one by one, the maximum joint temperature corresponding to the edge of each pulse also rises one by one, after reaching the peak junction temperature, the rise also causes common faults of power electronic devices.

Compared with the real-time temperature prediction technology of power electronic devices made of semiconductor materials, when the wave type duty cycle changes, the duty cycle decreases, and the duty cycle decreases, the junction temperature moves into a regular constant amplitude fluctuation, and the constant amplitude fluctuation of the junction temperature achieves a stable balance between heat generation and loss.

2.1.5. Establishment of the prediction equation

Because the temperature of the power supply is difficult to measure, it is more convenient to measure the temperature of the radiator, and there is a strong conversion relationship between the ambient temperature of the power supply and the temperature of the radiator. Because of this, we can do this by using the radiator temperature, specific, specific analysis. The process of the temperature of the heater is a very unstable stochastic process and can be calculated according to the following formula. Refer to **Figure 8** for the prediction structure of the equation.

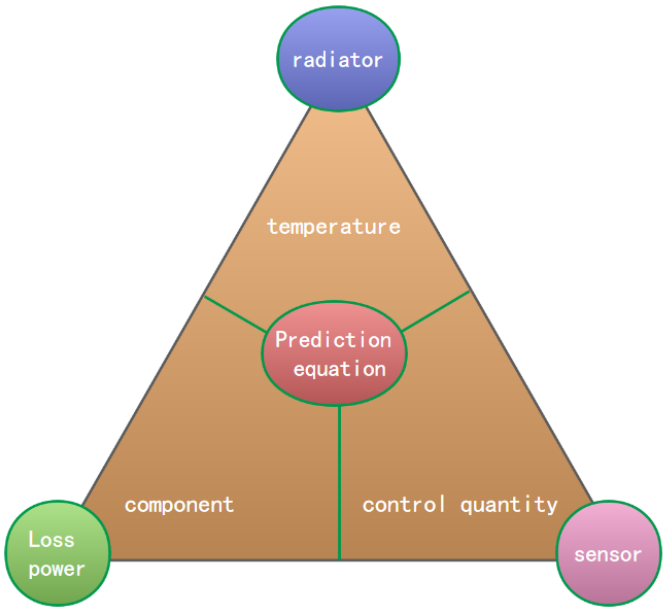

Figure 8. The predicted structure of the Equation.

In power supply temperature prediction, the prediction equation is established through the radiator temperature. Let the power supply temperature T_k be the state variable r_k and the radiator temperature be the observation variable. The state prediction equation and observation equation are as follows:

$$T_k = \Phi T_{k-1} + \Gamma w_k + \mathrm{B}u_k \tag{6}$$

Φ is the state transition matrix,Γ is the disturbance coefficient matrix, w_k is the ambient temperature change, u_k is the control quantity, and is the control coefficient matrix.

Observation equation:

$$r_k = \mathrm{H}T_{k-1} + n_k \tag{7}$$

H is the observation matrix, n_k is the observation noise.

The parameters for the case study in this paper are designed as follows **Table 5**:

Table 5. Model parameter settings.

Parameter	Symbol	Value/Description
initial temperature	T_0	25 ℃
Environmental temperature changes	w_k	0.5 ℃
Control quantity	u_k	0
State transition matrix	Φ	0.9
Disturbance coefficient matrix	Γ	0.1
Observation matrix	H	1
Observation noise	n_k	n_k~N(0,1)

2.2. State prediction and estimation

2.2.1. Necessity for state prediction and estimation

With too many interference factors, the main circuit voltage, will also change with the factors. For example, in the case of frequency converter change, the main circuit current under two different working frequency is often not equal, sometimes even in a constant power working frequency band, as the current change, the main circuit voltage, will constantly change, the specific numerical calculation formula for:

$$V_K = E_m - I_r \tag{8}$$

(V_K main circuit voltage, r is equivalent resistance, I for current). With the load in the source, the flow will follow more and more, but the voltage will be in turn, when the flow will reach the peak, the voltage of the main circuit will slowly at a minimum at this time. Not only that, for different power supply systems or different types of input circuits, the selection of equivalent resistance can not be established, coupled with the switching power supply being unstable, the load is still shaking back and forth, random disturbance and other uncertain factors are also difficult to determine. Using Kalman filter algorithm, accurately for the next working frequency point voltage value, can use the prediction estimation method to measure and predict current voltage, according to the statistical characteristics of voltage changes and the limitation of any conditions, can predict working frequency voltage, it can not only predict value, also can predict accurate voltage measurement anytime and anywhere, improve the precision [23]. As shown in **Figure 9**.

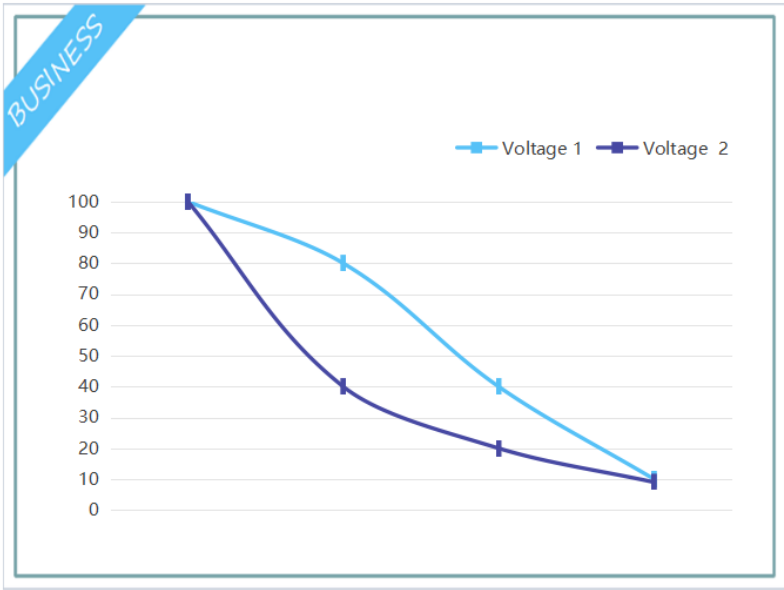

Figure 9. Main circuit voltage test.

2.2.2. Relationship between biological thermal response and electronic device thermal management

The characteristics of biomechanical and biomolecular markers reflect the response mechanisms of biological systems to external stress, temperature fluctuations, and damage. The parallels between thermal stress, vibration, and long-term fatigue issues in the operation of electronic and electrical equipment and thermal and mechanical stress in biological systems provide opportunities for cross-disciplinary applications.

Electronic devices are prone to damage under extreme temperatures, high loads, or prolonged operation. Traditional methods for equipment evaluation typically rely on physical sensors and numerical analysis. However, the pursuit of more refined approaches to predict failures or optimize design has become a key research focus. The rapid response mechanisms of biological systems to thermal and mechanical stress offer innovative inspiration for advancements in equipment monitoring and diagnostics.

A) Impact of biological thermal response on electronic device design

Biological thermal response is a critical consideration in the design of electronic devices, as the thermal properties of biological tissues directly influence the thermal design of the device. When designing wearable devices, the thermal conductivity of human skin and muscle tissues are key parameters, and the heat conduction equation ($q = -k\nabla K$) can be used to calculate the heat flux density (qq) at the interface between the device and biological tissues, thereby optimizing the heat dissipation design. The thermal damage threshold (T_{damage} = 41 ℃) is the upper limit for device design; exceeding this temperature may cause cellular damage. The Thermal Comfort Index (TCI) is used to evaluate the thermal comfort of the device, typically requiring TCI < 0.1TCI < 0.1. The TCI is calculated as follows:

$$\text{TCI} = \frac{T_{\text{skin}} - T_{\text{comfort}}}{\Delta T_{\text{max}}} \tag{9}$$

B) Thermal management and cellular molecular activities of electronic devices

The thermal management of electronic devices can draw inspiration from the thermal regulation mechanisms of biological cells. Cells protect themselves under high-temperature conditions by expressing Heat Shock Proteins (HSPs). Similarly, electronic devices can employ intelligent thermal management systems to prevent overheating by monitoring temperature (T) in real-time and adjusting heat dissipation strategies. Key parameters in thermal management systems include heat capacity (C), thermal resistance (R), and thermal time constant ($\tau = RC$). The temperature change of the device can be predicted using the heat balance equation ($C\frac{\mathrm{d}T}{\mathrm{d}t} = P - q$), where P is the device power consumption and q is the heat dissipation power. The safe temperature threshold (T_{safe} = 45 ℃) is the design target for the system, while the number ofthermal cycles ($N_{\mathrm{cycle}} = \frac{\sum \Delta T_i}{\Delta T_{\mathrm{max}}}$) must also be considered to assess long-term reliability.

C) Application of biomechanics in electronic devices

Biomechanical principles play a significant role in the design of electronic devices, particularly in wearable and implantable devices. By simulating the mechanical properties of human tissues, the mechanical design of devices can be optimized. For example, the elastic modulus of skin (E_{skin} = 0.1 MPa) and muscle tissues (E_{muscl} = 0.5 MPa) are key design parameters. The stress distribution (σ) at the interface between the device and biological tissues can be calculated using the stress-strain relationship ($\sigma = E\epsilon$), thereby optimizing the mechanical compatibility of the device. The Pressure Distribution Index (PDI $= \frac{\sum(\sigma_i - \sigma_{\mathrm{avg}})^2}{N}$) is used to evaluate the uniformity of pressure distribution, typically requiring PDI < 0.2.

3. Results

3.1. Kalman filter based parameter prediction

The temperature at the next time step can be predicted as follows:

$$T_1 = 0.9 \times 25 + 0.1 \times 0.5 + 0 = 22.55\ ℃ \tag{10}$$

Observing the temperature of the radiator:

$$r_1 = 1 \times 22.55 + n_1 \approx 22.55\ ℃ \tag{11}$$

Repeat the above steps to obtain the temperature change trend, as shown in the **Table 6** below:

Table 6. Temperature trend.

Time Step k	T_{k-1}	w_k	u_k	T_k	r_k
1	25.0	0.5	0	22.55	22.55
2	22.55	0.5	0	20.345	20.345
3	20.345	0.5	0	18.3605	18.3605
4	18.3605	0.5	0	16.57445	16.57445
5	16.57445	0.5	0	14.966905	14.966905
6	14.966905	0.5	0	13.520214	13.520214

Table 6. (*Continued*).

Time Step k	T_{k-1}	w_k	u_k	T_k	r_k
7	13.520214	0.5	0	12.218193	12.218193
8	12.218193	0.5	0	11.046374	11.046374
9	11.046374	0.5	0	9.9917366	9.9917366
10	9.9917366	0.5	0	9.0425629	9.0425629
11	9.0425629	0.5	0	8.1883066	8.1883066
12	8.1883066	0.5	0	7.4194759	7.4194759

3.2. Fusion prediction and estimation

The multi-sensor fusion theory is to "merge" the data from several information sources through a certain optimization algorithm to create more reliable and accurate information, that is, an optimal estimator in the relevant state is given according to the multi-source observation information. Because the accuracy of each sensor is unlikely to be exactly the same, in order to make the fusion results better, the corresponding weight coefficient can be explored according to the measurement value obtained by each sensor so as to achieve the optimal fusion conclusion, namely the so-called weight calculation fusion optimization algorithm. For several sensors on the same parameter measurement, a weight calculation fusion may optimize the algorithm. This is to find the weighted average of the data obtained by each sensor. Only by the measurement data provided by the sensor, the minimum data with the root mean square error can be fused, so the distribution of weights is very obvious harm to the fusion effect. The dispatch is appropriate, the fusion effect is obvious, the dispatch is not scientific, and the accuracy and stability of the system is not improved. The sensor measures a condition, the measurement data of the sensor is unknown; the two are not associated with each other and are unbiased estimates; the measurement standard deviation means the accuracy of the sensor, the accuracy of the sensor. According to the definition of the weighted average data fusion method, the postfusion state estimation is the characteristic function of the current sensor coefficient [24].

(1) Sensor measurement model

Assume there are n sensors measuring the same state x, and the measurement value of each sensor is:

$$z_i = x + v_i \ (i = 1,2,3,\cdots,n) \tag{12}$$

where:

z_i is the measurement value of the i-th sensor;

x is the true state (unknown);

v_i is the measurement noise of the i-th sensor, assumed to be zero-mean Gaussian noise with variance σ^2, that is, $v_i \sim N(0, \sigma^2)$.

The fused state estimate $\hat{x}$ can be expressed as the weighted average of the measurement values from each sensor:

$$x = \frac{\sum_{i=1}^{n} w_i z_i}{\sum_{i=1}^{n} w_i} \tag{13}$$

where:

w_i is the weight of the i-th sensor;
the weights satisfy the normalization condition: $\sum_{i=1}^{n} w_i = 1$.

Lagrange Multiplier Method for Weight Optimization: In order to minimize the error variance under the weight normalization condition, we construct the Lagrange function:

$$\mathcal{L}(w_1, w_2, w_3, \cdots, w_n, \lambda) = \sum_{i=1}^{n} {w_i}^2 {\sigma_i}^2 + \lambda(1 - \sum_{i=1}^{n} w_i) \tag{14}$$

where λ is the Lagrange multiplier.

(2) Fused state estimate: By substituting the weights into the weighted average formula, we obtain the fused state estimate:

$$\hat{x} = \sum_{i=1}^{n} w_i z_i = \frac{\sum_1^n z_i/{\sigma_i}^2}{\sum_1^n 1/{\sigma_i}^2} \tag{15}$$

where w_i is the weight obtained through the optimization using the Lagrange multiplier method.

The above simulation results show that when the discrete system continuous discrete variable Kalman filter and the optimal weight calculation data preprocessing are closely combined, several sensors of the Kalman filter device speed value can be used as a comprehensive measurement accuracy, in addition, even if there is a poor accuracy speed value in the combination, the final speed is very obvious, the composition of these algorithms is also applicable to other multi-sensor system software measurement.

3.3. State prediction and estimation

Equations (5) and (6) can be used for prediction and estimation calculation, and the algorithm block diagram is shown in **Figure 10**. According to the estimated value and the time value, the error value is obtained, and then the factor correction of the error value is obtained, and the timing of the investigation makes the prediction accurate. Finally, use it again to estimate the voltage value for the next operation. After power-on, the inverter does not start, and the power value is the highest. After the inverter is started, the voltage drops, and the data must be retrieved, updated and saved at each start. After the start of operation, the DC voltage of the main circuit can be measured, which can be calculated by the formula:

$$v_0 = \frac{v_0 - v_1}{T}, v_1 = z_1 \tag{16}$$

(z_1 the main circuit DC voltage, T is the time, v_0 and v_1 the voltage at different times). After the multiple increase, the starting operation will end. As shown in **Figure 10**.

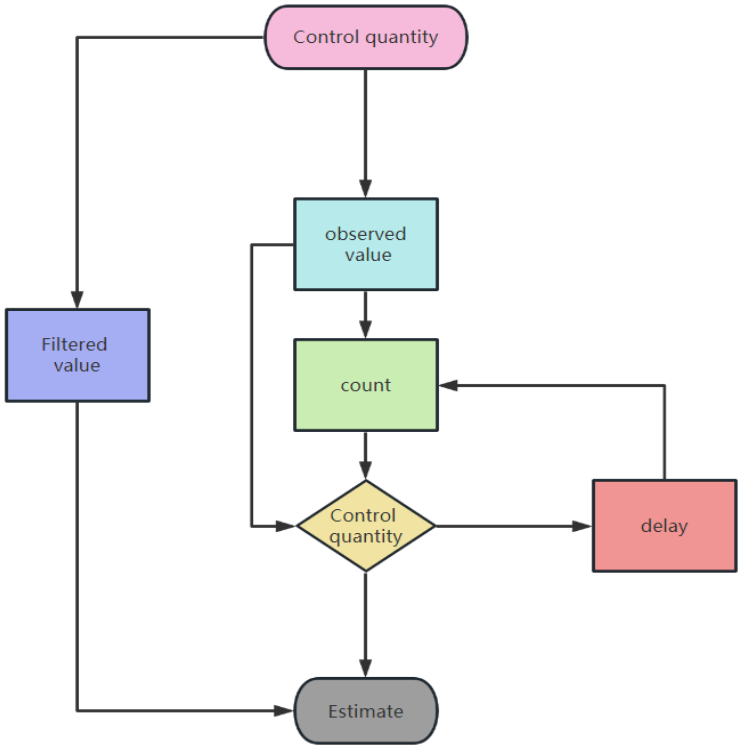

Figure 10. Schematic representation of the prediction and estimation algorithm.

In experimental manipulation, the change plot of the detected voltage is indicated by thin solid lines, and thick solid lines indicate the predicted analysis voltage plot. The starting frequency is 20 Hz, and when the curve is more than 20 Hz, it almost coincides, confirming that the accuracy of the prediction algorithm is relatively high. The prediction algorithm determines the accuracy of the derived voltage. When the compressor starts, the voltage drops significantly, and then the signal frequency increases. It is obvious that this decrease is not linear; thus the voltage-derived accuracy is increasingly pronounced [25].

Therefore, it can be seen from the program, experimental data and trial run results that the output voltage accuracy can be significantly improved by using the main circuit voltage prediction method without voltage feedback. Due to the recursive algorithm, the software cost is very small, but the application value is relatively high. Even with the voltage feedback, the algorithm can greatly improve the system stability and accuracy.

3.4. Monitoring electronic device status using biomolecular markers

Biomolecular marker technology can be used to develop new sensors for monitoring the operational status of electronic devices. For example, the expression level of Heat Shock Proteins (HSP) can serve as a biological indicator of thermal effects. Sensor design must consider the detection sensitivity (SS) and specificity (Sp) of biomolecules. The concentration of biomolecules (C) can be calculated using the biomolecular concentration equation ($K = k[S]$), where (k) is the proportionality constant and [S] is the sensor signal. Biomolecular marker technology can also provide additional biological indicators, such as cell viability ($V_{\text{cell}} = f(T, t)$) and tissue

damage level ($D_{\text{tissue}} = g(T,t)$), to evaluate the safety and reliability of the device. Refer to **Table 7** for simulation parameters of the biothermal reaction.

Table 7. Simulation parameters for biological thermal response.

Index	Unit	Value
Heat Shock Protein (HSP) Expression Level	ng/mL	0.15
Device Temperature	℃	40
Biomolecular Detection Sensitivity	ng/mL	0.1
Biomolecular Detection Specificity	%	95
Proportionality Constant	ng/mL·℃	0.05
Device Temperature Range	℃	T_{min} = 35 ℃; T_{max} = 45℃
Thermal Damage Threshold	℃	T_{damage} = 41 ℃; T_{safe} = 45 ℃
Safe Temperature Threshold	℃	45
Cell Viability	%	$V_{\text{cell}} = 100\% - 2\% \times (T - 37)$
Tissue Damage Level	%	$D_{\text{tissue}} = 0.5\% \times (T - 37)^2$

In this study, the expression level of Heat Shock Proteins (HSPs) is calculated using the biomolecular concentration equation:

$$[\text{HSP}] = k \times (T - 37) = 0.05 \times (40 - 37) = 0.15 \text{ ng/mL} \quad (17)$$

The cell viability is calculated using the following formula:

$$V_{\text{cell}} = 100\% - 2\% \times (40 - 37) = 100\% - 6\% = 94\% \quad (18)$$

Calculation of tissue damage degree:

$$D_{\text{tissue}} = 0.5\% \times (40 - 37)^2 = 0.5\% \times 9 = 4.5\% \quad (19)$$

During the thermal effect assessment process, if $T \geq T_{\text{damage}}$, a warning signal will be issued. If $T \geq T_{\text{safe}}$, trigger the emergency cooling mechanism. Send a warning signal.

Sensor output:

Detected HSP concentration: $[\text{HSP}] = 0.15$ ng/mL;

Cell viability: $V_{\text{cell}} = 94\%$;

Degree of organizational damage: $\text{D}_{\text{tissue}} = 4.5\%$.

Device temperature 40 ℃ is below the thermal damage threshold of 41 ℃, but close to the safety temperature threshold of 45 ℃; cell viability is 94%, indicating that the device has little impact on the surrounding biological tissues; the degree of tissue damage is 4.5%, within the acceptable range; the HSP concentration detected by the sensor is 0.15 ng/mL, indicating that the device has a low thermal effect on biological tissues.

4. Conclusion

Using Kalman filter prediction estimation method, study, estimate and predict the parameters of power equipment, the best, through the preset state parameters, better avoid high-temperature damage power equipment fault can solve the output voltage

accuracy in complex environment: at the same time, the Kalman filter state prediction technology combined with innovative, overvoltage or overcurrent, short circuit and overheating protection measures, can greatly improve the reliability of power electronic equipment to reach a new level.

The integration of biological thermal response and electronic device thermal management offers new insights for device design. By incorporating biological heat conduction models and heat shock protein (HSP) monitoring, the thermal effects of devices on biological tissues can be assessed in real-time, optimizing heat dissipation strategies. This interdisciplinary approach not only improves the thermal management efficiency of devices but also enhances their safety and reliability in biological environments.

Incorporating biomechanical and biomolecular markers into the evaluation of electronic device operational states not only offers a novel perspective for reliability studies but also provides valuable insights for the integration of biological and engineering technologies. Future advancements in this field hold the potential to enable more intelligent and efficient methods for device monitoring and design.

This paper is designed for the various problems encountered in the current engineering practice. The Kalman filter technology and biomolecular markers are implemented in operation can greatly reduce the probability of power electronic failure, which is a new control technology with high practical value. In short, we should pay enough attention to the reliability of electronic equipment. We need to combine the specific engineering practice, and constantly put forward new ideas and methods, to ensure the safe and reliable operation of energy facilities, which is the direction of our future efforts.

Author contributions: Conceptualization, JL; methodology, PZ; software, PZ; validation, JL; formal analysis, JL; investigation, PZ; resources, PZ; data curation, PZ; writing—original draft preparation, JL; writing—review and editing, JL; visualization, JL; supervision, JL; project administration, PZ; funding acquisition, PZ. All authors have read and agreed to the published version of the manuscript.

Funding: This work was supported by Project of Hebi Institute of Engineering and Technology, Henan Polytechnic University No.2023-JGZD-006.

Ethical approval: Not applicable.

Conflict of interest: The authors declare no conflict of interest.

References

1. Jalili-Jahani N, Zeraatkar E. Fuzzy wavelet network based on extended Kalman filter training algorithm combined with least square weight estimation: Efficient and improved chromatographic QSRR/QSPR models. Chemometrics and Intelligent Laboratory Systems. 2021; 208: 104191.
2. Li C, Ma J, Yang Y, Gan Y. Low complexity adaptive volume Kalman filter algorithm (Chinese). Journal of Beijing University of Aeronautics and Astronautics. 2022; 48(4): 716–724.
3. Liu Y, Yang F, Liang Z, Yang J. Echo cancellation algorithm in STFT domain based on Kalman filter (Chinese). Acoustic technology. 2022; 41(5): 757–762.
4. Li Y, Dong G, Chen K, et al. Analysis of passive location accuracy based on Kalman filter (Chinese). Journal of Missile and Guidance. 2022; 42(4): 43–46.

5. Alnak DE, Karabulut K. Effect of Arc Shaped Bar on Heat Transfer and Fluid Characteristics at Cooling of Electronic Equipment. Journal of Engineering Thermophysics. 2020; 29(4): 657–673.
6. Hussain A, Ahmed Z, Shafiq M, et al. An Adaptive Denoising Algorithm for Online Condition Monitoring of High-Voltage Power Equipment. Electric Power Components and Systems. 2020; 48(9–10): 1036–1048.
7. Abdulle A, Garegnani G, Zanoni A. Ensemble Kalman filter for multiscale inverse problems. Multiscale modeling & simulation. 2020; 18(4): 1565–1594.
8. Rehman A, Shahid H, Afzal MA, Bhatti HMA. Accurate and Direct GNSS/PDR Integration Using Extended Kalman Filter for Pedestrian Smartphone Navigation. Gyroscopy and Navigation. 2020; 11(2): 124–137.
9. D'Amore L, Cacciapuoti R, Mele V. A scalable Kalman filter algorithm: Trustworthy analysis on constrained least square model. Concurrency and computation: Practice and experience. 2021; 33(4): e6022.
10. Hernandez-Barragan J, Rios JD, Alanis AY, et al. Adaptive Single Neuron Anti-Windup PID Controller Based on the Extended Kalman Filter Algorithm. Electronics. 2020; 9(4): 636.
11. Jia M, Rolandi M. Soft and ion-conducting materials in bioelectronics: From conducting polymers to hydrogels. Advanced healthcare materials. 2020; 9(5): 1901372.
12. Dechiraju H, Jia M, Luo L, Rolandi M. Ion-conducting hydrogels and their applications in bioelectronics. Advanced Sustainable Systems. 2022; 6(2): 2100173.
13. Wang L, Liu W, Yan Z, et al. Stretchable and shape-adaptable triboelectric nanogenerator based on biocompatible liquid electrolyte for biomechanical energy harvesting and wearable human–machine interaction. Advanced Functional Materials. 2021; 31(7): 2007221.
14. Liu M, Qian F, Mi J, Zuo L. Biomechanical energy harvesting for wearable and mobile devices: State-of-the-art and future directions. Applied Energy. 2022; 321: 119379.
15. Cho S, Yun Y, Jang S, et al. Universal biomechanical energy harvesting from joint movements using a direction-switchable triboelectric nanogenerator. Nano Energy. 2020; 71: 104584.
16. Wang R, Du Z, Xia Z, et al. Magnetoelectrical clothing generator for high-performance transduction from biomechanical energy to electricity. Advanced Functional Materials. 2022; 32(6): 2107682.
17. Liang L, Yan Y, Wang C, et al. GRACE-FO attitude data reconstruction based on Kalman filter (Chinese). Journal of Geophysics. 2022; 65(12): 4602–4615.
18. Liu M, Peng Y, Qu S, et al. Improved quadratic correlation moving location method combined with Kalman filter (Chinese). Fire and Command and Control. 2022; 47(10): 140–144.
19. Qiu R, Li J, Li X, et al. Trajectory prediction based on Kalman filter algorithm (Chinese). Television technology. 2022; 46(6): 24–28.
20. Tang H, Jiang J. Research on the influence of extended Kalman filter on the tracking performance of time-varying parameters (Chinese). Journal of Nanjing University of Aeronautics and Astronautics. 2022; 54(2): 304–310.
21. Tariq SL, Ali HM, Akram MA, Janjua MM. Experimental investigation on graphene based nanoparticles enhanced phase change materials (GbNePCMs) for thermal management of electronic equipment. Journal of Energy Storage. 2020; 30: 101497.
22. Tatematsu A, Motoyama H, Tanigawa A. Application of the FDTD-based simulation code VSTL REV to the lightning surge analysis of a nuclear power plant. Electric Power Systems Research. 2020; 178: 106040.
23. Wang Y, Zhu C, Zhao S. FDIA detection method based on adaptive Kalman filter (Chinese). Computer Application and Software. 2022; 39(4).
24. Yildiz R, Barut M, Demir R. Extended Kalman filter based estimations for improving speed-sensored control performance of induction motors. IET electric power applications. 2020; 14(12): 2471–2479.
25. Zhang Z, Schuerhuber R, Fickert L, et al. Systematic stability analysis, evaluation and testing process, and platform for grid-connected power electronic equipment. Elektrotechnik und Informationstechnik. 2021; 138(1): 20–30.